

## Article

# The Effect of Cellulose Fibre Length on the Efficiency of an Intumescent Flame Retardant System in Poly(lactic acid)

Kata Enikő Decsov , Bettina Ötvös, Thuy Tien Thanh Nguyen  and Katalin Bocz \* 

Department of Organic Chemistry and Technology, Faculty of Chemical Technology and Biotechnology, Budapest University of Technology and Economics, Műegyetem rkp. 3, H-1111 Budapest, Hungary

\* Correspondence: bocz.katalin@vbk.bme.hu

**Abstract:** In the flame retardancy of the biopolymer matrix and natural fibre reinforcement containing green composites, researchers face multiple challenges, such as low thermal stability, the candlewick effect of fibres and compatibility issues. Cellulosic fibres have been shown to have char-promoting properties and to advantageously interact with intumescent systems. In this work, melamine-polyphosphate was combined with neat or flame-retardant-treated cellulosic fibres differing in fibre length to obtain intumescent flame retarded poly(lactic acid) composites. The effect of the cellulose fibre length was evaluated in both forms. The structure-property relationships were evaluated by thermal and flammability test methods. It was found that the formation and the structure of the fire-protecting char are influenced by the length of the cellulose fibres, and thus it noticeably affects the effectiveness of the flame-retardant system. Cellulose fibres with an average length of 30–60  $\mu\text{m}$  were found to contribute the best to the formation of an integrated fibrous-intumescent char structure with enhanced barrier characteristics.

**Keywords:** cellulose; fibre length; intumescence; poly(lactic acid); melamine polyphosphate



**Citation:** Decsov, K.E.; Ötvös, B.; Nguyen, T.T.T.; Bocz, K. The Effect of Cellulose Fibre Length on the Efficiency of an Intumescent Flame Retardant System in Poly(lactic acid). *Fire* **2023**, *6*, 97. <https://doi.org/10.3390/fire6030097>

Academic Editor: Ali Cemal Benim

Received: 31 January 2023

Revised: 22 February 2023

Accepted: 28 February 2023

Published: 2 March 2023



**Copyright:** © 2023 by the authors. Licensee MDPI, Basel, Switzerland. This article is an open access article distributed under the terms and conditions of the Creative Commons Attribution (CC BY) license (<https://creativecommons.org/licenses/by/4.0/>).

## 1. Introduction

Improving the properties of poly(lactic acid) (PLA) by incorporating biofillers is a favourable method for maintaining its biodegradability [1–3]. There is extensive research on the mechanical properties of composites of biopolymers and natural fibres, especially with cellulose, the most abundant of all, which can be isolated from most plants, such as wood, bamboo and cotton [4]. The addition of cellulose to alter the properties of PLA [5] and the interfacial compatibility improvement [6] are often in focus, but there is still a lack of knowledge on the flame retardancy of these multiphase materials. In the flame retardancy of the biopolymer matrix and natural fibre reinforcement containing green composites, researchers must face the challenges of low thermal stability [7] and candlewick effect [8,9] of the fibres, as well as their compatibility [10] issues.

Over the past ten years, researchers have been studying the effects of natural cellulose-containing fibres [11–15], micro- [16–18] and nano-scale [19–23] cellulose additives [24–26]. As the better flame retardancy depends on both the loading rate and the dispersion state of the filler [27], Kaci et al. [24] compared neat microcrystalline cellulose (MCC) to cellulose nanowhiskers (CNW) in the PLA matrix, in the presence of PLA-grafted-maleic anhydride as a compatibiliser. They found that both the aspect ratio and the filler content affect the fire retardancy properties of PLA/cellulosic fibres. It was observed in Pyrolysis Combustion Flow Calorimeter (PCFC) testing that at the lower loading level of 1%, the CNW was more efficient in increasing the temperature of the peak heat release rate (pHRR) and decreasing the pHRR value. However, at the filler content of 3%, there was a significant difference as both size forms decreased the pHRR value by 9% at most. The morphological investigation of the multifilament yarns performed under Scanning Electron Microscopy (SEM) [25] indicated that CNW with a

higher aspect ratio and a smaller size had better compatibility with PLA than MCC, and thus could be more homogeneously dispersed in the matrix.

When MCC was combined with tricresyl phosphate, their synergistic effect in PLA resulted in an outstanding improvement in the impact strength and flame retardancy of the composites [28]. From an industrial point of view, minimizing the amount of flame-retardants with increased biofiller content can be beneficial in terms of cost and improving the mechanical properties. To determine the optimal formulation, Matsumoto et al. [18] concluded that the dehydration temperature of the biofiller must be lower than the degradation temperature of the neat polymer, and when assisted with ammonium polyphosphate (APP), the dehydration of cellulose should start at approximately 95 °C less than the degradation temperature of the neat polymer for enabling the formation of sufficient non-flammable gas and char layer.

Various phosphorus-treated cellulosic materials were synthesised and investigated in PLA. When natural cellulose fibres (CF) were treated with diammonium-phosphate (DAP), the best flame retardancy results were observed for the fibre treatment with a 5% DAP solution [14]. When CF was coated with resorcinol bis (diphenyl phosphate) (RDP), as low as 8 wt% of the RDP-coated CF in the PLA matrix sufficed to pass the UL-94 test with a V-0 rating, reach a limiting oxygen index (LOI) of 28% and significantly decreasing the average heat release rates and the pHRR values [16]. A core-shell nanofibrous flame-retardant system was created by Feng et al. [22] via in situ chemical grafting of diethyl phosphite onto the high-strength cellulose nanofibre surface. When incorporated at the loading amount of 10% into PLA, the sample obtained a V-0 rating while simultaneously enabling a significant reduction in the pHRR, by 31% [22]. Cellulose nanocrystals (CNC) were incorporated in PLA along with N,N'-diallyl-phenylphosphoricdiamide (P-AA) and achieved an LOI of 28.8%, a V-0 rating in the UL-94 test. However, in the cone calorimetry, the flame retarded samples could not achieve a significant improvement compared to the neat PLA, as P-AA was observed to mainly have a flame inhibition effect in the gas phase [21]. Phosphazene-containing CNC was synthesised to balance the adverse impact on the performance attributed to CNC's low onset decomposition temperature. The optimal composition of 7% APP and 3% phosphazene-containing CNC had the best results in PLA, such as having the highest LOI of 28.1%, the lowest pHRR and the V-0 rating in the UL-94 test [23].

The combination of phosphate and nitrogen-containing materials as flame-retardant treating agents for cellulosic materials has been known for decades [28–30]. Recent studies have also investigated this interaction; Nam et al. [31] achieved excellent flame-retarded greige cotton nonwoven fabric by applying DAP with the addition of urea (U) for treatment. They showed that urea increased the decomposition temperature of the fabric and accelerated the decomposition of glycosyl units of the cellulose. Bocz et al. [32] optimised the ratio of DAP and urea (U) on plain-woven flax fabric and investigated the fibre-matrix interaction as a function of the amount and distribution of flame-retardant additives in flax fabric reinforced PLA composites. In their research, the DAP:U ratio of 1:1 in 10 w/v% aqueous solution was found to be optimal for the FR treatment of flax fabrics.

Recently, it has been demonstrated that the dimensions and specific surface area of the charring agents are crucial regarding the interaction with the intumescent system [33]. Costes et al. investigated the effect of combining MCC or CNC with aluminium phytate in PLA, where the charring effect was enhanced in both cases. CNC's high specific surface area proved beneficial in promoting the formation of a better insulating charred layer [26].

This study investigated the effects of the length of micro-sized neat and FR-treated cellulose particles in an intumescent flame-retardant system in the PLA matrix, respectively. Our goal was to determine the fibre length that favours the enforcement of the candle wick effect and which fibre length can advantageously affect the barrier properties of the intumescent carbonaceous layer.

## 2. Materials and Methods

### 2.1. Materials

The PLA matrix was an Ingeo™ Biopolymer 4032D type from NatureWorks LLC (Minnetonka, MN, USA). For melamine polyphosphate (MPP), BUDIT® 341 Budenheim was used as a base flame-retardant. Arbocel UFC 100, BE 600/30, B600 and BC200 type cellulose fibres from CTS Europe (Mildenhall, UK) were used as co-additives. The length and width data of these cellulose fibres can be found in Table 1. For the flame-retardant surface treatment (FR) of the cellulose fibres, diammonium phosphate (DAP) and urea (U) were used and purchased from Sigma-Aldrich Co. (St. Louis, MO, USA).

**Table 1.** The trade names, average fibre lengths and thicknesses of the applied cellulose fibres. The sample names were given based on their average lengths.

Additive Name	Trade Name	Length [ $\mu\text{m}$ ]	Thickness [ $\mu\text{m}$ ]
C8	Arbocel UFC 100	8	2
C30	Arbocel BE 600/30	30	18
C60	Arbocel B 600	60	20
C300	Arbocel BC 200	300	20

### 2.2. Flame Retardant Treatment of the Cellulose Fibres

For the flame-retardant treatment, the cellulose fibres were immersed in the aqueous solution of diammonium phosphate (DAP) and urea (U) with a ratio of 1:1 and a concentration of 10  $w/v\%$ , for 10 min. The composition of the treating solution was determined based on the results of our previous research study [32]. After the soaking, the fibres were filtered, dried overnight at 80 °C, and powdered before compounding.

### 2.3. Preparation of Flame-Retarded PLA Composites

#### 2.3.1. Preparation of Composites

The flame-retarded PLA composites were mixed in a Brabender Plasti-Corder Lab-Station (Brabender GmbH & Co. KG, Duisburg, Germany) internal mixer. Before mixing, all the components were dried at 80 °C for 6 h. For the compounding procedure, the chamber temperature was 185 °C, the rotor speed was 50 rpm, and the total mixing time was 5 min. First, the PLA granules were mixed until fully melted, and then the MPP and the cellulose additives were added. For reference materials, neat PLA and only MPP-containing PLA samples were prepared. Table 2 shows the composition of the manufactured PLA composites.

**Table 2.** Formulations of the PLA composites in the experiments.

Sample Name	PLA%	MPP%	Cellulose Type	Cellulose%
For fibre quantity experiments				
PLA	100	-	-	-
PLA + MPP	85	15	-	-
PLA + MPP + 5% C300	80	15	C300	5
PLA + MPP + 10% C300	75	15	C300	10
PLA + MPP + 15% C300	70	15	C300	15
For fibre length experiments				
PLA	100	-	-	-
PLA + MPP	85	15	-	-
PLA + MPP + C8	75	15	C8	10
PLA + MPP + C30	75	15	C30	10
PLA + MPP + C60	75	15	C60	10
PLA + MPP + C300	75	15	C300	10
PLA + MPP + FR-C8	75	15	FR-C8	10
PLA + MPP + FR-C30	75	15	FR-C30	10
PLA + MPP + FR-C60	75	15	FR-C60	10
PLA + MPP + FR-C300	75	15	FR-C300	10

### 2.3.2. Sample Moulding

The melt-mixed materials were hot-pressed into 3 mm thick plates using a Teach-Line Platen Press 200E (Dr. Collin GmbH, Munich, Germany) type heated hydraulic press at 180 °C and 100 bars. The LOI and UL-94 flammability test specimens were obtained by cutting the plates with a saw.

## 2.4. Characterisation

### 2.4.1. FTIR Spectroscopy

The additives were analysed using a Bruker Tensor 37 (Bruker Corporation, Billerica, MA, USA) type Fourier transform infrared spectrometer (FTIR) with an ATR unit in attenuated total reflectance (ATR) mode (4000–600  $\text{cm}^{-1}$ ) with a resolution of 4  $\text{cm}^{-1}$  and 32 scan accumulation.

### 2.4.2. Scanning Electron Microscopy

Scanning electron microscopic (SEM) images of the additives were taken with a JEOL 6380LVa (JEOL, Tokyo, Japan) type apparatus in a high vacuum. The accelerating voltage was 10–15 keV. The samples were fixed by conductive double-sided carbon adhesive tape and sputtered with gold by a JEOL 1200 ion sputter (JEOL, Tokyo, Japan).

### 2.4.3. Thermogravimetric Analysis

TA Instruments Q5000 apparatus (TA Instruments LLC, New Castle, NH, USA) was used for the TGA measurements. The nitrogen flow rate was set to 25 mL/min. Samples of the additives and the composites were positioned in platinum pans. The samples were heated from room temperature to 800 °C at a 10 °C/min rate. The extrapolated onset temperature was determined according to the ISO 11358-1 standard, which defines it as the point of intersection of the starting-mass baseline and the tangent to the TGA curve at the maximum gradient point.

### 2.4.4. Limiting Oxygen Index

Limiting oxygen index (LOI) measurements were performed according to the ISO 4589 standard using a Fire Testing Technology Ltd. (East Grinstead, UK) apparatus.

### 2.4.5. UL-94

The UL-94 standard flammability tests were carried out according to ISO 9773. The samples were 3 mm thick, and 5 specimens were tested for each composition.

### 2.4.6. Mass Loss Calorimetry (MLC)

A Fire Testing Technology Ltd. (East Grinstead, UK) instrument was used according to ISO 13927 standard for the mass loss calorimetric measurements. Specimens  $100 \times 100 \times 3 \text{ mm}^3$  in size were tested under 35  $\text{kW/m}^2$  heat flux. The main combustion characteristics, such as the heat release rate (HRR) as a function of time, the time to ignition (TTI), the total heat release (THR) and the peak heat release rate (pHRR), were obtained. The remaining mass residue values were read at the moment of flame out, as they are influenced by the fact that the longer the measurement continues after the flame extinction, the more the residual carbon layer degrades. In many cases, the data collecting continued for a long time until the heat emission curves returned to near zero. Two parallel measurements were performed where the pHRR and THR values were reproducible within  $\pm 10\%$ .

### 2.4.7. Raman Spectroscopy

Raman spectra were recorded with a LabRAM (Horiba Jobin Yvon) instrument with a  $\lambda = 532 \text{ nm}$  Nd-YAG laser source (40 mW nominal laser power). A filter of 0.6 OD was used to decrease the excitation beam intensity, in turn reducing the chance of sample degradation. LabSpec 6 software was applied for data collection and parameter optimisation. The exposure time was 60 s per point. The collected spectra were truncated from

800 to 2000  $\text{cm}^{-1}$  for spectral analysis. After the background correction and normalisation of the spectra, they were deconvoluted with BWF and Lorentzian line pair [34] for the G and D peaks, respectively, with the Origin program.

### 3. Results and Discussion

#### 3.1. Investigation of the Effect of Fibre Quantity

The composite samples were prepared with 15% MPP and 5, 10 and 15% additive C300, the longest-fibre-length cellulose, to find the optimal composition where the cellulosic fibres contribute the best to the fire-protective effectiveness of the carbonaceous layer.

##### 3.1.1. TGA Results of the Fibre Quantity Experiment

The C300 type cellulose containing PLA composites were analysed in TGA. The recorded thermograms are presented in Figure 1, while the obtained thermal characteristics are presented in Table 3. As expected, the cellulose fibres decreased the thermal stability of the PLA composites due to the early depolymerisation and the thermal cleavage of polysaccharides in the cellulose by transglycosylation at about 300 °C [35]. The TGA results also indicate that cellulose addition results in increased char yields. In this respect, the highest cellulose content (15%) is the most beneficial.

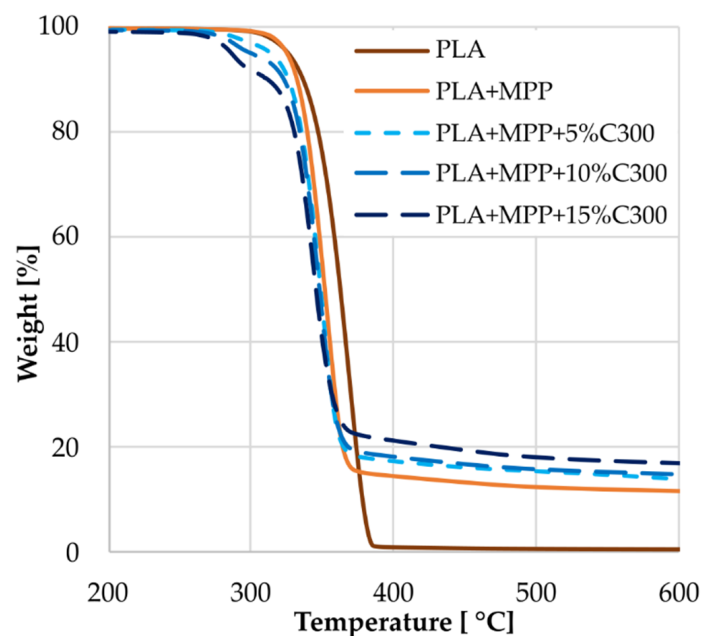


**Figure 1.** TGA results of the C300 containing PLA samples.

**Table 3.** TGA results of the composite samples with different neat cellulose content.

Sample	T <sub>Onset</sub> [°C]	T <sub>MAX Decomp</sub> [°C]	Slope Max Decomp [%/°C]	Residue @600 °C [%]
PLA	344	368	2.74	0.6
PLA + MPP	334	353	2.80	11.7
PLA + MPP + 5% C300	330	350	2.73	14.0
PLA + MPP + 10% C300	329	348	2.62	14.9
PLA + MPP + 15% C300	325	343	2.43	17.0

##### 3.1.2. Limiting Oxygen Index Values of the Composite Samples

Although the cellulose fibre addition increases the char yield based on the TGA results (Figure 1), the flammability of these composites slightly increased, as reflected by the

measured LOI values, shown in Table 4. The lower LOI values of the cellulose-containing composites compared to that of the PLA + MPP sample can be explained by the candlewick effect of the natural fibres [9,13]. The cellulose fibres have higher thermal conductivity compared to the PLA, and thus they can transmit heat below the burning region and speed flammable mass to the burning area, resulting in the candlewick effect. Nevertheless, the amount of cellulose added (at least in the range of 5–15%) did not significantly affect the LOI results.

**Table 4.** LOI values of the composite samples with differing neat cellulose content.

Sample	LOI [%]
PLA	21.0
PLA + MPP	27.0
PLA + MPP + 5% C300	25.0
PLA + MPP + 10% C300	25.0
PLA + MPP + 15% C300	25.5

### 3.1.3. Mass Loss Calorimetry Results

The PLA composites with increasing cellulose (C300) contents were also characterised by mass loss type calorimetry (MLC). The recorded heat release rate curves are presented in Figure 2, while the corresponding combustion characteristics are summarised in Table 5. It can be seen that the presence of cellulose shortens the TTI of the PLA composites, which is attributed to the early decomposition of cellulose at around 300 °C [35], as also indicated by the TGA results (Figure 1). In addition, longer burning times were measured for all the cellulose-containing samples, likely because the cellulose fibres are prone to glow.

To evaluate the effect of the different cellulose fibre quantities, analysis of variance (ANOVA) was performed with Statistica (TIBCO Software Inc. 3307 Palo Alto, CA, USA) software. These results indicated that the quantity of the added cellulose significantly influenced the pHRR values ( $p$ -value = 0.01337, significance level: 5%). Making post-hoc investigations with Fisher's Least Significant Difference (LSD) test, it was confirmed with a pairwise comparison that the 10 and 15% C300-containing samples significantly differ from the PLA + MPP and the 5% cellulose-containing sample. However, the difference between the 10 and 15% samples' pHRR values was insignificant.

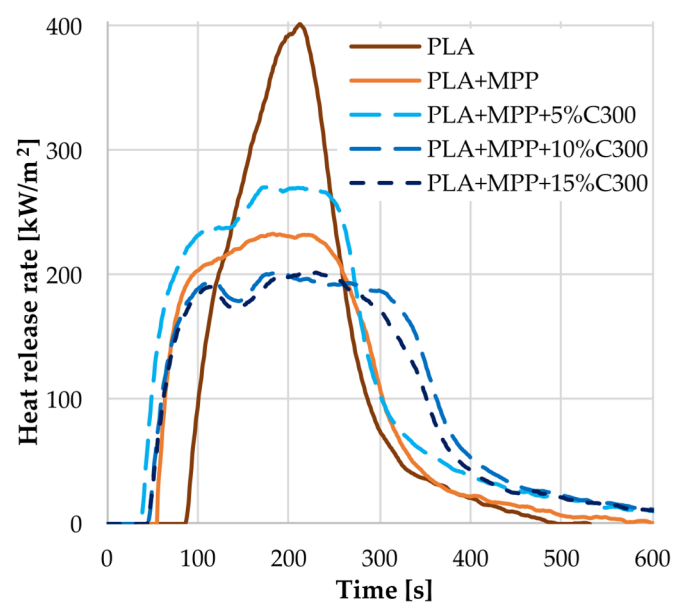


**Figure 2.** Heat release rate curves of the samples with different neat cellulose content.

**Table 5.** Average mass loss calorimetry results of the composite samples with different neat cellulose content.

Sample Name	pHRR [kW/m <sup>2</sup> ]	t <sub>pHRR</sub> [s]	THR [MJ/m <sup>2</sup> ]	t <sub>ign</sub> [s]	t <sub>flaming</sub> [s]	Residue @Flame Out [%]
PLA	392	225	64	93	233	2.3
PLA + MPP	245	233	58	54	280	12.4
PLA + MPP + 5% C300	267	182	64	36	349	9.3
PLA + MPP + 10% C300	192	197	59	44	342	15.8
PLA + MPP + 15% C300	194	232	54	44	310	18.8

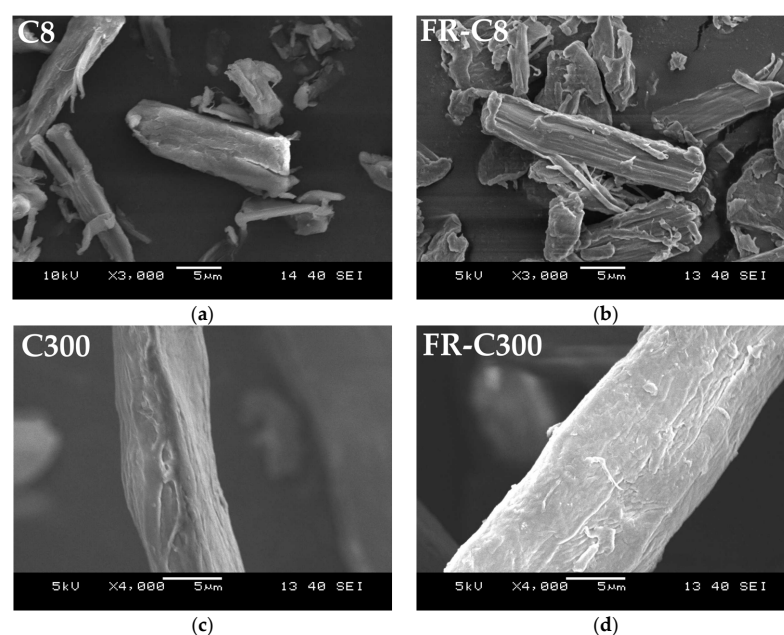
Based on the MLC results, the formation of the so-called “char-bonded” structure, as proposed by Horrocks [36], could be observed. This finding indicates that a sufficient amount of cellulose fibre can effectively improve the physical integrity and barrier characteristics of the carbonaceous layer formed by MPP, which is reflected by the reduced pHRR values of the composites at 10 and 15 wt% cellulose contents. At 5% cellulose, however, this effect cannot prevail yet, and the lower amount of cellulose fibres was found to degrade the char structure, accompanied by increased pHRR and THR values and the reduced mass of the combustion residue. The beneficial “char-bonded” structure arose first at 10% C300 fibre content. Above this content, the further reduction in the heat emission and increased charred residue could be achieved.

### 3.2. Characterisation of the Cellulose Fibres

The cellulose fibres, differing in fibre length, were used in neat and FR-treated forms in the PLA composites. Before incorporation, the fibres were characterised by morphological, spectroscopic and thermal analyses.

#### 3.2.1. SEM Analysis

The surface of the cellulose fibres was examined in SEM before and after the FR treatment. The images obtained from the neat and treated fibres with an average length of 8 (C8) and 300  $\mu\text{m}$  (C300) are shown in Figure 3. Based on the images, the FR treatment did not noticeably modify the morphology of the fibres.

**Figure 3.** SEM images of the (a) Untreated C8 additive; (b) FR-treated C8 additive; (c) untreated C300 additive; (d) FR-treated C300 additive.

### 3.2.2. FTIR Analysis

The ATR-FTIR spectra collected on the FR-treated cellulose fibres confirmed the presence of FR active compounds on the surface. In Figure 4, the presence of urea is confirmed as the twin peaks of a broad band at 3200 to 3600  $\text{cm}^{-1}$  and at 1600–1650  $\text{cm}^{-1}$  from the N-H group stretching vibrations, as well as the absorption band for the C=O group at 1700  $\text{cm}^{-1}$  and the C-N asymmetric stretching at 1454  $\text{cm}^{-1}$ , appear in the spectra of the FR-treated cellulose fibres. The shoulder at 3270  $\text{cm}^{-1}$  corresponds to the N-H vibration in  $\text{NH}_4$  and indicates the presence of DAP on the surface of the treated fibres.

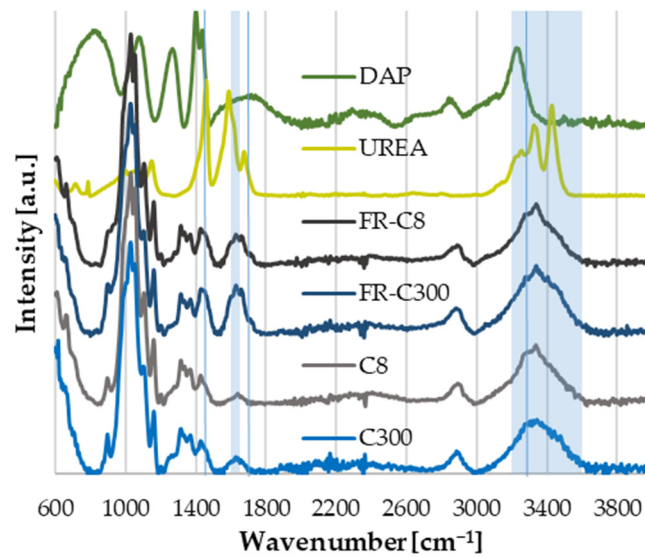


Figure 4. ATR-FTIR spectra of C8 and C300 before and after FR-treatment.

### 3.2.3. TGA Curves of the Cellulose Fibres

TGA thermograms of the neat and FR-treated cellulose fibres, mainly differing in length, were taken, and the thermal characteristics are summarised in Table 6. It is apparent that the FR treatment dramatically increased the mass of the charred residue obtained at 600 °C. This is attributed to the effective dehydration of cellulose by the phosphorus-containing fire retardant (DAP) that leads to water release, enhanced char formation and a reduced amount of flammable gases. Furthermore, the FR treatment reduced the dehydration temperature of the cellulosic fibres by approximately 80–100 °C. Based on the lower dehydration temperature of cellulose against the decomposition of the neat polymer, the improved fire retardancy of the FR-treated cellulose-containing PLA composites could be expected [18]. Considering the effect of the fibre length, in the case of neat cellulose fibres, the longer fibres yield more residues at 600 °C. This effect disappears after the FR treatment; therefore, no clear trend can be identified. For the untreated C8 fibre, the slightly lower onset temperature and residual weight could be attributed to the effect of the specific chemicals (or their remains) used in the fine fibre production.

Table 6. TGA measurement data of the untreated and FR-treated cellulose additives.

Additive Name	T <sub>Onset</sub> [°C]	T <sub>max degr</sub> [°C]	Slope [%/°C]	Residue @600 °C [%]
C8	313	336	2.49	2.5
C30	325	352	2.04	8.3
C60	316	349	1.71	10.4
C300	324	353	2.04	9.6
FR-C8	236	263	1.09	35.7
FR-C30	242	273	1.12	34.4
FR-C60	236	274	0.91	33.9
FR-C300	225	262	0.76	36.7

### 3.3. Investigation of the Effect of Cellulose Fibre Length

Based on the results of the fibre quantity experiments, in addition to the 15% MPP, the neat and FR-treated cellulose loading level of 10% was chosen to be used in the experiments where the effects of the cellulose fibre length were investigated and evaluated in the PLA

#### 3.3.1. TGA of the PLA Composites with Different Cellulose Fibre Length

As can be seen in Figure 5 and Table 7, the decomposition of the cellulose-containing composites starts at lower temperatures than those of pure PLA and PLA + MPP. The weight loss occurring between 200 and 300 °C can be attributed to the dehydration of the cellulose fibres and their interaction with MPP, accompanied by the generation of nonflammable gases and char formation.

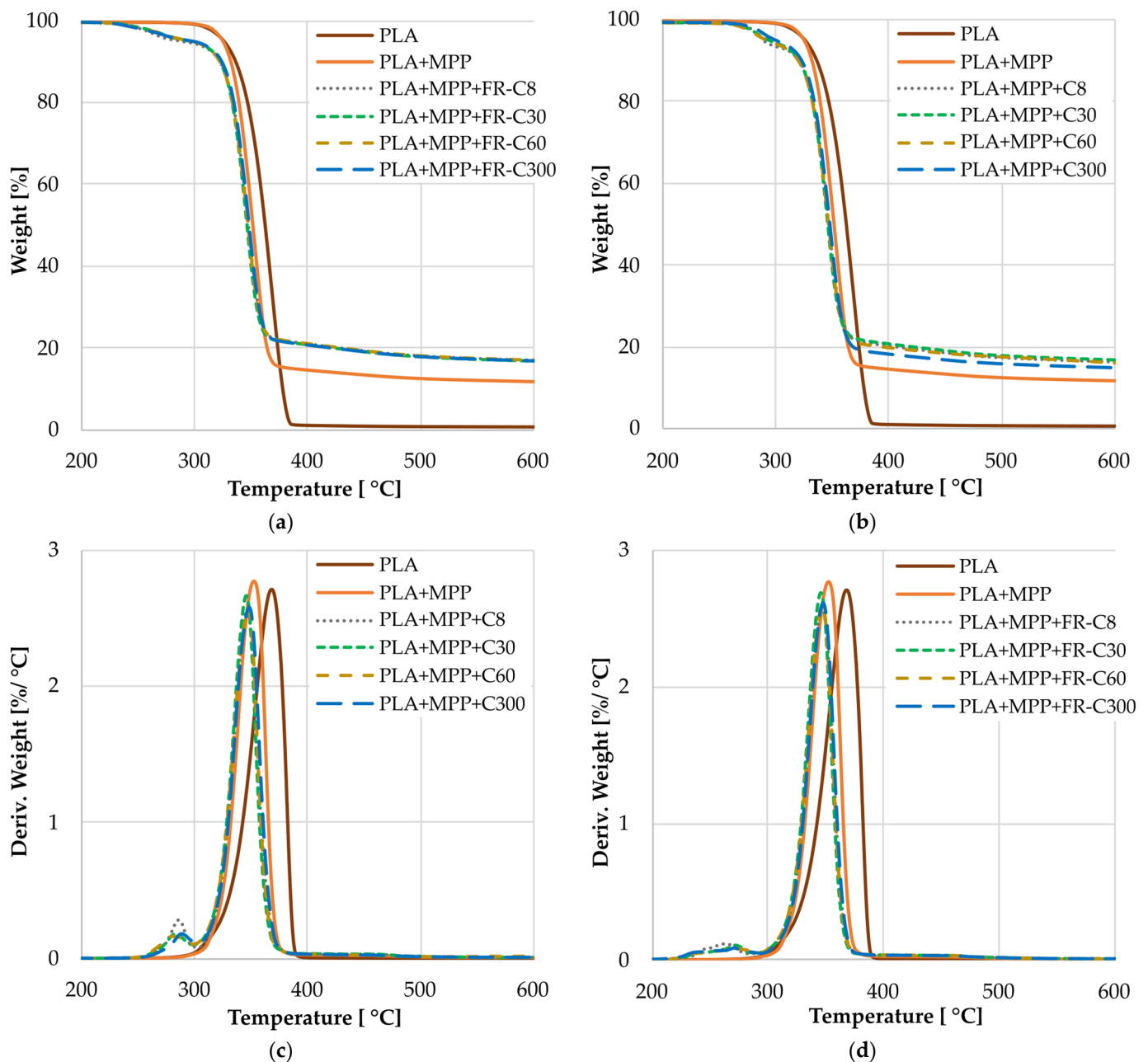


**Figure 5.** TGA curves of the composites with (a) untreated cellulose additives and (b) FR-treated cellulose additives; and the DTG curves of the (c) untreated cellulose additives and (d) FR-treated cellulose additives.

**Table 7.** TGA results of the composites samples with differing cellulose fibre length.

Sample	T <sub>dehydr</sub> [°C]	Slope <sub>dehydr</sub> [%/°C]	T <sub>Onset</sub> [°C]	T <sub>max decomp</sub> [°C]	Slope <sub>decomp</sub> [%/°C]	Residue @600 °C [%]
PLA	-	-	344	368	2.74	0.6
PLA + MPP	-	-	332	351	2.64	12.1
PLA + MPP + C8	286	0.25	328	346	2.64	16.3
PLA + MPP + C30	282	0.20	328	346	2.70	16.8
PLA + MPP + C60	280	0.17	327	347	2.62	16.1
PLA + MPP + C300	288	0.19	329	348	2.62	14.9
PLA + MPP + FR-C8	263	0.12	329	347	2.67	17.0
PLA + MPP + FR-C30	272	0.11	328	346	2.72	16.8
PLA + MPP + FR-C60	270	0.10	328	347	2.64	17.0
PLA + MPP + FR-C300	271	0.10	330	348	2.66	16.8

This decomposition step shifted to even lower temperatures when the FR-treated cellulose fibres were used. The second decomposition step in the temperature range of 310 and 380 °C is where the decomposition of PLA and MPP takes place, while the third decomposition step corresponds to the thermal degradation of the char. The slightly increased amount of charred residue obtained for the PLA composites with the FR-treated cellulose, compared to those with the untreated fibres, is also associated with acid-catalysed, low-temperature dehydration [18,32]. In TGA, the length of the cellulose fibres did not noticeably affect the thermal decomposition behaviour of the composites.

### 3.3.2. LOI and UL94 of the PLA Composites with Different Cellulose Fibre Length

The flammability test results of the cellulose-containing PLA composites are presented in Table 8. At 15% MPP and 10% cellulose content, independently from the FR-treatment, flaming dripping occurred during vertical burning. A better classification than V-2 could not be reached in the UL-94 test due to the candlewick effect and the high flammability of the cellulose fibres. The applied FR-treatment could not completely eliminate the heat and flame transmission along the fibres. It must be noted that the interfacial adhesion between the flame-retardant, the fibre and the polymer also influences the flame-retardant performance. The FR-treatment of the fibres often hinders the fibre-matrix interaction, resulting in an adverse effect on the flame-retardant properties [9,20,32]. The weaker interfacial bonding between the FR-treated fibres and the PLA matrix is proposed to be more pronounced when shorter, high-surface-area fibres are used. Namely, when the C8 fibre was used in FR-treated form, the LOI value of the PLA composite reduced compared to the neat form (from 27.5% to 26.5%), while in the case of larger fibre size, the FR-treatment imparted higher LOI values to the composites.

**Table 8.** LOI and UL-94 test results of the composite samples with differing cellulose fibre length.

Sample	LOI [%]	UL-94	Sample	LOI [%]	UL-94
PLA	20.5	H.B.	PLA + MPP	27	V2
PLA + MPP + C8	27.5	V2	PLA + MPP + FR-C8	26.5	V2
PLA + MPP + C30	26.0	V2	PLA + MPP + FR-C30	26.5	V2
PLA + MPP + C60	26.0	V2	PLA + MPP + FR-C60	26.5	V2
PLA + MPP + C300	25.5	V2	PLA + MPP + FR-C300	25.5	V2

In addition, as a function of the increasing cellulose fibre length, a decreasing tendency of the LOI values among the PLA composites was observed, which may be attributed to the fibre length (and alignment) dependence of the candlewick effect; the longer fibres can transmit the heat more effectively below the burning zone. However, this trend became less apparent when the cellulose fibres were used in FR-treated form, indicating that the FR treatment reduced the flame transmission along the fibres. In the case of the longest

C300-type cellulose, the FR treatment was insufficient to overcome the candlewick effect and could not improve the flame retardancy of the composite. This was also confirmed by the fact that, in the case of FR-C8, the three min LOI condition was met first, while in the case of the longer fibres, the 5 cm length condition was fulfilled first.

### 3.3.3. Mass Loss Calorimetry Results of the PLA Composites with Differing Cellulose Fibre Length

The heat release rate curves recorded during the mass loss calorimeter tests of the PLA composites are presented in Figure 6, while the combustion characteristics are given in Table 9. The shape of the HRR curves of the cellulose-containing composites is typical for thick charring materials [37]. It is apparent that the longer cellulose fibres (C60 and C300) are more effective in flattening the HRR curves and reducing the pHRR values (Table 9). It is proposed that fibres with a higher aspect ratio can have a reinforcing effect on the intumescent char, thereby improving the compactness and both the thermal and mechanical stability of the fire-protecting layer. According to Table 9, the cellulose fibre length does not seem to have much effect on the THR of the composites. Similar conclusions were drawn by Ghazzawi et al. [38], who found a negligible effect of the fibre length of fibres with low thermal conductivity on the fire performance of fibre-reinforced polymer composites.

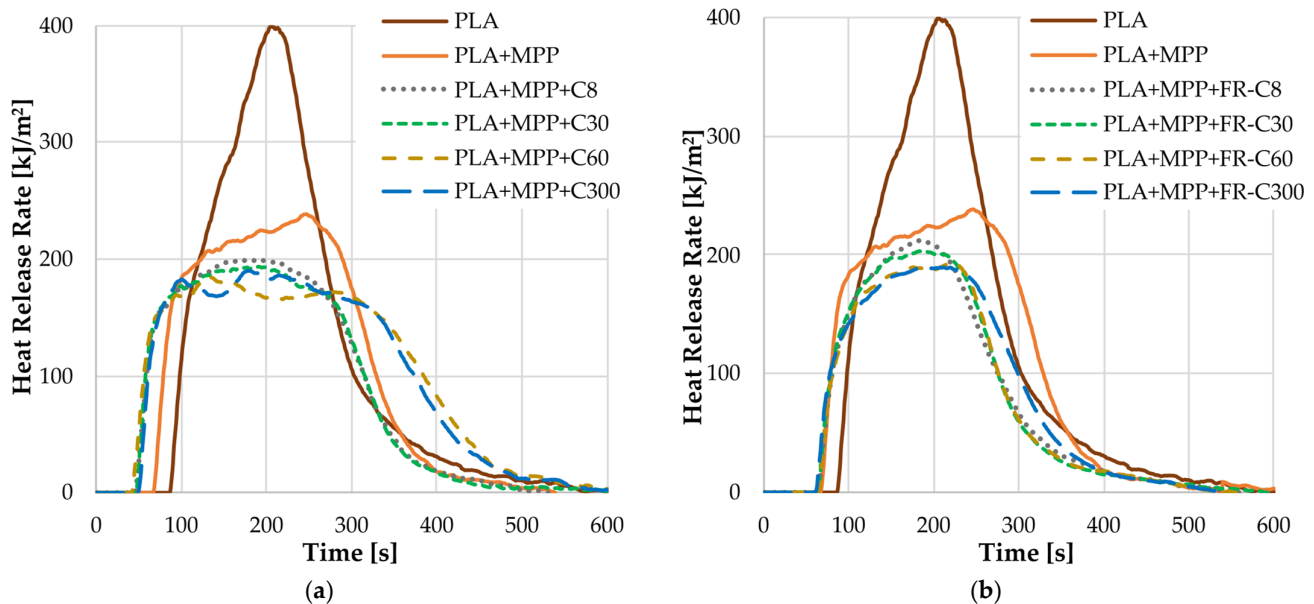


**Figure 6.** Heat release rate curves of the composites with (a) untreated cellulose additive; (b) FR-treated cellulose additives.

**Table 9.** Average mass loss calorimetric results of the PLA composite samples with different cellulose fibre length.

Sample Name	pHRR [kW/m <sup>2</sup> ]	t <sub>pHRR</sub> [s]	THR [MJ/m <sup>2</sup> ]	t <sub>ign</sub> [s]	t <sub>flaming</sub> [s]	Residue @Flame out [%]
PLA	392	225	64	93	325	2.3
PLA MPP	245	233	58	54	334	12.4
PLA + MPP + C8	205	216	55	43	380	13.6
PLA + MPP + C30	187	168	50	44	330	16.3
PLA + MPP + C60	185	149	52	46	402	15.2
PLA + MPP + C300	192	197	59	44	386	15.8
PLA + MPP + FR-C8	213	210	42	59	317	14.2
PLA + MPP + FR-C30	195	172	40	62	283	15.9
PLA + MPP + FR-C60	193	224	41	54	285	15.7
PLA + MPP + FR-C300	192	185	43	55	302	14.8

The FR treatment of the cellulosic fibres resulted in a slight increase in the peak heat release rate values of the composites. However, it increased the time to ignition and noticeably shortened the combustion time, as well as reducing the total heat emission (Table 9). The improved barrier characteristics of the corresponding chars are attributed to two factors: (1) The phosphorus-induced dehydration of the cellulose fibres that produces a substantial amount of water and char; (2) The beneficial interaction between the carbonaceous structure of cellulose and the intumescent char.

#### 3.3.4. SEM Images of the Char Residues

Figure 7 presents the SEM micrographs taken from the charred residues of the cellulose-free PLA + MPP sample and of the composites containing neat and FR-treated C60 and C300 additives, respectively. It can be seen that MPP resulted in the formation of a charred web structure with holes of 200–300  $\mu\text{m}$  in diameter (Figure 7a). The SEM analyses served as evidence for the formation of “char-bonded” structures in the case of all the cellulose-containing composites. It can be seen in Figure 7b that the cellulose fibres with an average fibre length of 60  $\mu\text{m}$  are well incorporated in the carbonised web structure. When the C60 type fibre was applied in FR-treated form, a coherent char structure was formed (Figure 7c), indicating increased interactions between the components. Such a compact char layer is a good insulator and oxygen barrier to block the degradation of the polymer, and thereby explains the observed improvement in the flame retardancy properties of the PLA + MPP + FR-C60 composite (Table 9).

However, the neat C300 fibres of larger particle size were found to partially break the uniform structure of the charred web (Figure 7d). Nevertheless, based on the SEM images presented in Figure 7e, the FR-treatment of the C300 fibres advantageously affected their physical and chemical interaction and generated a more coherent char. The improvement in the char structure is well reflected by the corresponding MLC results, i.e., the noticeably reduced THR was measured for the PLA + MPP + FR-C300 composite compared to the PLA + MPP + C300 counterpart.

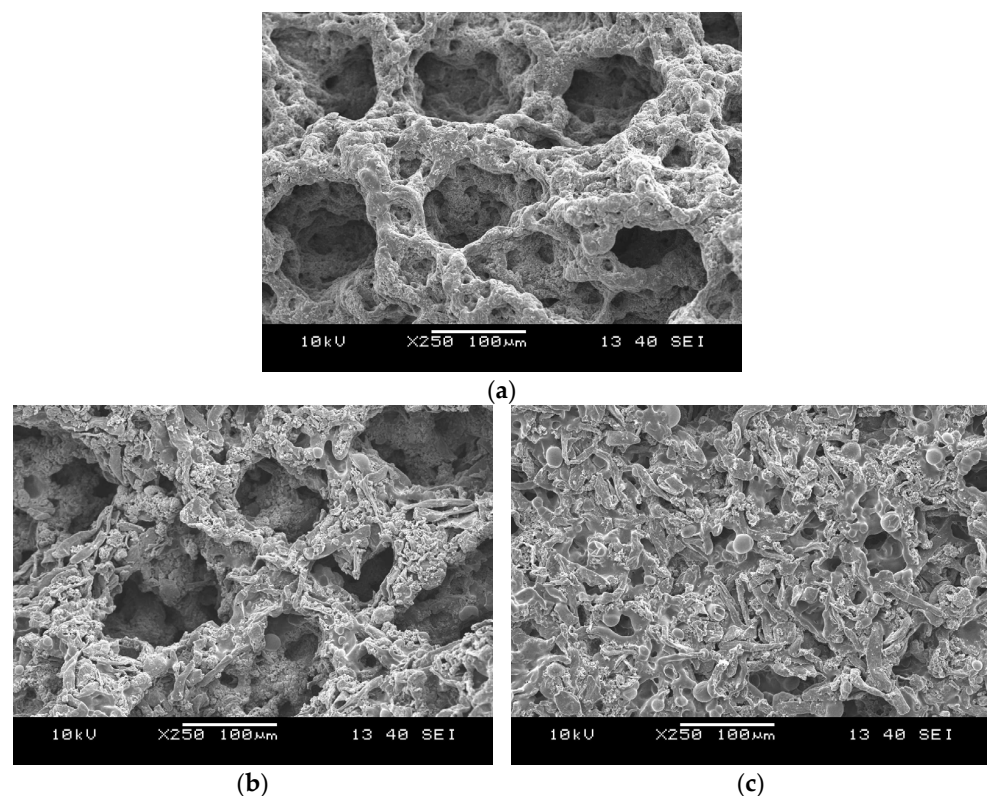
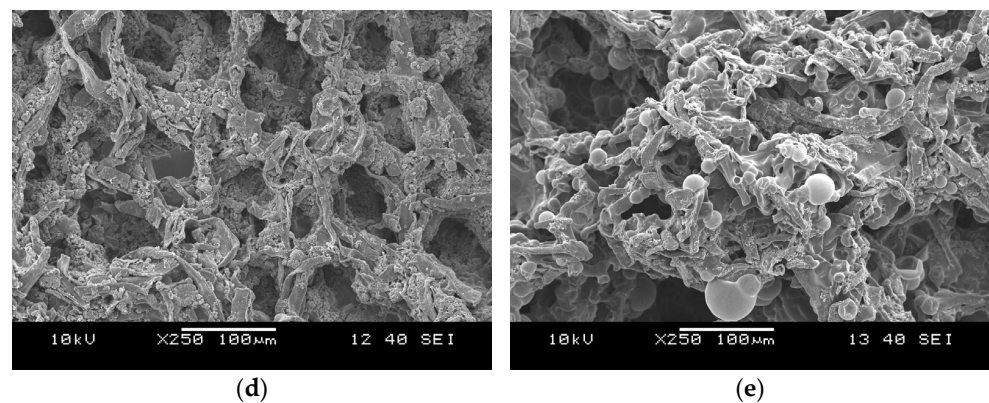


Figure 7. Cont.



**Figure 7.** SEM images of the charred residues of; (a) PLA + MPP, (b) PLA + MPP + C60, (c) PLA + MPP + FR-C60, (d) PLA + MPP + C300, (e) PLA + MPP + FR-C300.

### 3.3.5. Raman Spectroscopic Analysis of the Char Residues

The charred residues of the best-performing cellulose-containing composites—the C60, C300, FR-C60 and the FR-C300—and samples containing only MPP were examined using Raman spectroscopy. It can be seen in Figure 8 that the analysed chars have two distinct vibration bands; namely, the D peak near  $1360\text{ cm}^{-1}$ , which is the mode of vibration of the carbon atom ( $\text{sp}^3$  hybridisation), and the G peak near  $1580\text{ cm}^{-1}$ , which is the  $2\text{E}_{2g}$  vibration of the C–C bond in graphite ( $\text{sp}^2$  hybridisation). The intensity ratio of these two bands is generally used to indicate the degree of the graphitisation of the char layer and to quantify the disorder or defects in the structure. It can be seen in Figure 8a that the intensity ratios differed depending on the samples. The  $A_D$  and  $A_G$  area values were calculated from the fitted D and G bands (Figure 8b). The smaller the value of  $A_D/A_G$ , the higher the degree of graphitisation and the more compact the char layer [39–41]. According to the results presented in Table 10, the cellulose fibres with smaller particle size (C60) are well incorporated into the carbonaceous structure, thus facilitating the formation of a more compact char layer. The graphitisation degrees of the chars with larger cellulose fibres (C300) are, however, similar to that of the only MPP-containing sample, indicating that longer cellulose fibres increase the number of defects in the graphitised char structure.

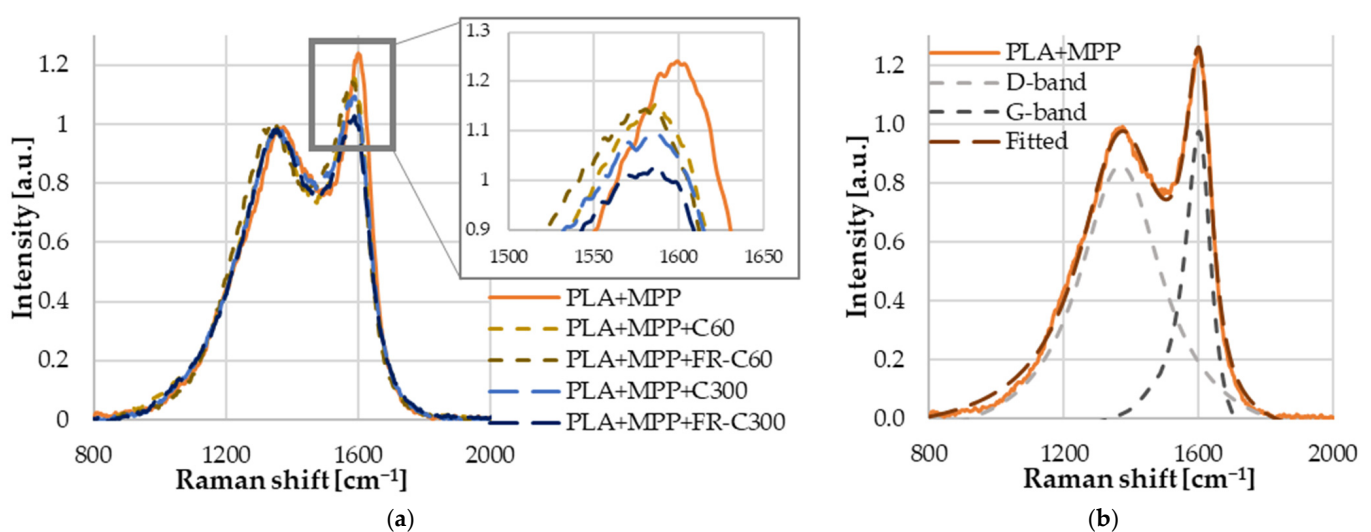


**Figure 8.** (a) Raman spectra of the charred composites normalised to the D-band; (b) Example of the fitted D and G bands on the Raman spectrum of PLA + MPP composite's char.

**Table 10.** Area ratios of the fitted D and G bands of the char residues.

Sample Name	A <sub>D</sub> /A <sub>G</sub>
PLA + MPP	2.18
PLA + MPP + C60	1.79
PLA + MPP + FR-C60	1.62
PLA + MPP + C300	2.05
PLA + MPP + FR-C300	2.11

#### 4. Conclusions

The addition of cellulose fibres to the intumescent flame-retarded PLA composite can be a promising way to strengthen the fire-protecting carbonaceous layer. It is crucial to optimise the proportion and the size of cellulosic fibres to create an effectively flame-retarded biocomposite.

While investigating the cellulose addition, in addition to using a constant amount (15%) of MPP in the PLA matrix, the enhanced char formation of the cellulose-containing composites was revealed in TGA. However, the char-promoting behaviour of the cellulose fibres was only shown in the combustion characteristic of the PLA composites when the fibre content was higher than 10%. At the same time, the candlewick effect of the cellulose fibres increased the flammability of the composites, which was reflected by the decreased LOI values. This adverse effect was found to accelerate with the increasing fibre length, as a 2.0% lower LOI value was measured for the PLA composite with C300 type cellulose (25.5%) compared to that with C8 fibres (27.5%). However, the longer fibres performed better during the mass loss calorimeter test in reducing the heat release rates of the composites. It is proposed that the higher surface area of the shorter cellulose fibres supports the chemical interactions with MPP, while for the longer fibres with a higher aspect ratio, the physical effects, i.e., the structural reinforcement of the intumescent char, come to the fore.

The FR treatment of the cellulose fibres with P- and N-containing compounds resulted in enhanced char formation and reduced flammable gas release during thermal decomposition. However, the FR treatment was ineffective in eliminating the candlewick effect of longer fibres (C300) and noticeably reducing the flammability of the composites. Nevertheless, the composites with FR-treated cellulose fibres had an increased ignition time, shorter flaming time and significantly (by about 20%) reduced total heat release during combustion in the mass loss calorimetry. The improved barrier characteristics of the char layers are related to the effective integration of the carbonised fibrous substances and the intumescent char, as evidenced by the SEM analysis of the combustion residues.

Regarding the overall fire-retardant performance of the intumescent system, the cellulose fibres with 30–60 µm length were found to be optimal. These fibres have only a moderate candlewick effect, while during combustion, they can effectively enhance the structural integrity of the fire-protecting carbonaceous layer.

**Author Contributions:** Conceptualisation, K.B. and K.E.D.; methodology, K.E.D. and K.B.; validation, K.E.D., K.B. and T.T.T.N.; formal analysis, B.Ö.; investigation, K.E.D. and B.Ö.; resources, K.B.; data curation, K.B. and T.T.T.N.; writing—original draft preparation, K.E.D.; writing—review and editing, T.T.T.N., B.Ö. and K.B.; visualisation, K.E.D.; supervision, K.B.; project administration, K.B.; funding acquisition, K.B. All authors have read and agreed to the published version of the manuscript.

**Funding:** The project was funded by the National Research, Development and Innovation Fund of Hungary in the frame of the 2019–1.3.1-KK-2019–00004 and GINOP\_PLUSZ-2.1.1-21-2022-00041 projects. The research was funded by the Hungarian Scientific Research Fund, grant number FK128352. K. Decsov was supported by the ÚNKP-22-3-II-BME-126 New National Excellence Program of the Ministry for Innovation and Technology from the source of the National Research, Development and Innovation Fund.

**Institutional Review Board Statement:** Not applicable.

**Informed Consent Statement:** Not applicable.

**Data Availability Statement:** The data presented in this study are available on request from the corresponding author.

**Conflicts of Interest:** The authors declare no conflict of interest.

## References

1. Getme, A.S.; Patel, B. A Review: Bio-Fiber's as Reinforcement in Composites of Polylactic Acid (PLA). *Mater. Today Proc.* **2020**, *26*, 2116–2122. [[CrossRef](#)]
2. Zhu, L.; Qiu, J.; Liu, W.; Sakai, E. Mechanical and Thermal Properties of Rice Straw/PLA Modified by Nano Attapulgite/PLA Interfacial Layer. *Compos. Commun.* **2019**, *13*, 18–21. [[CrossRef](#)]
3. Zhou, L.; Ke, K.; Yang, M.-B.; Yang, W. Recent Progress on Chemical Modification of Cellulose for High Mechanical-Performance Poly(lactic acid)/Cellulose Composite: A Review. *Compos. Commun.* **2021**, *23*, 100548. [[CrossRef](#)]
4. Chen, W.; Yu, H.; Lee, S.-Y.; Wei, T.; Li, J.; Fan, Z. Nanocellulose: A Promising Nanomaterial for Advanced Electrochemical Energy Storage. *Chem. Soc. Rev.* **2018**, *47*, 2837–2872. [[CrossRef](#)] [[PubMed](#)]
5. Khosravi, A.; Fereidoon, A.; Khorasani, M.M.; Naderi, G.; Ganjali, M.R.; Zarrintaj, P.; Saeb, M.R.; Gutiérrez, T.J. Soft and Hard Sections from Cellulose-Reinforced Poly(lactic acid)-Based Food Packaging Films: A Critical Review. *Food Packag. Shelf Life* **2020**, *23*, 100429. [[CrossRef](#)]
6. Ren, Z.; Guo, R.; Bi, H.; Jia, X.; Xu, M.; Cai, L. Interfacial Adhesion of Polylactic Acid on Cellulose Surface: A Molecular Dynamics Study. *ACS Appl. Mater. Interfaces* **2020**, *12*, 3236–3244. [[CrossRef](#)]
7. le Bras, M.; Duquesne, S.; Fois, M.; Grisel, M.; Poutch, F. Intumescent Polypropylene/Flax Blends: A Preliminary Study. *Polym. Degrad. Stab.* **2005**, *88*, 80–84. [[CrossRef](#)]
8. Chen, D.; Li, J.; Ren, J. Combustion Properties and Transference Behavior of Ultrafine Microencapsulated Ammonium Polyphosphate in Ramie Fabric-Reinforced Poly(L-Lactic Acid) Biocomposites. *Polym. Int.* **2011**, *60*, 599–606. [[CrossRef](#)]
9. Shumao, L.; Jie, R.; Hua, Y.; Tao, Y.; Weizhong, Y. Influence of Ammonium Polyphosphate on the Flame Retardancy and Mechanical Properties of Ramie Fiber-Reinforced Poly(lactic acid) Biocomposites. *Polym. Int.* **2010**, *59*, 242–248. [[CrossRef](#)]
10. Zhang, J.-F.; Sun, X. Mechanical Properties of Poly(lactic acid)/Starch Composites Compatibilized by Maleic Anhydride. *Biomacromolecules* **2004**, *5*, 1446–1451. [[CrossRef](#)]
11. Suparanon, T.; Phetwarotai, W. Fire-Extinguishing Characteristics and Flame Retardant Mechanism of Polylactide Foams: Influence of Tricresyl Phosphate Combined with Natural Flame Retardant. *Int. J. Biol. Macromol.* **2020**, *158*, 1090–1101. [[CrossRef](#)] [[PubMed](#)]
12. Vahabi, H.; Shabanian, M.; Aryanasab, F.; Mangin, R.; Laoutid, F.; Saeb, M.R. Inclusion of Modified Lignocellulose and Nano-Hydroxyapatite in Development of New Bio-Based Adjuvant Flame Retardant for Poly(lactic acid). *Thermochim Acta* **2018**, *666*, 51–59. [[CrossRef](#)]
13. Boczk, K.; Szolnoki, B.; Marosi, A.; Tábi, T.; Wladyka-Przybylak, M.; Marosi, G. Flax Fibre Reinforced PLA/TPS Biocomposites Flame Retarded with Multifunctional Additive System. *Polym. Degrad. Stab.* **2014**, *106*, 63–73. [[CrossRef](#)]
14. Suardana, N.P.G.; Ku, M.S.; Lim, J.K. Effects of Diammonium Phosphate on the Flammability and Mechanical Properties of Bio-Composites. *Mater. Des.* **2011**, *32*, 1990–1999. [[CrossRef](#)]
15. Kandola, B.K.; Mistik, S.I.; Pornwannachai, W.; Anand, S.C. Natural Fibre-Reinforced Thermoplastic Composites from Woven-Nonwoven Textile Preforms: Mechanical and Fire Performance Study. *Compos. B Eng.* **2018**, *153*, 456–464. [[CrossRef](#)]
16. Guo, Y.; He, S.; Zuo, X.; Xue, Y.; Chen, Z.; Chang, C.-C.; Weil, E.; Rafailovich, M. Incorporation of Cellulose with Adsorbed Phosphates into Poly(lactic acid) for Enhanced Mechanical and Flame Retardant Properties. *Polym. Degrad. Stab.* **2017**, *144*, 24–32. [[CrossRef](#)]
17. Zhu, T.; Guo, J.; Fei, B.; Feng, Z.; Gu, X.; Li, H.; Sun, J.; Zhang, S. Preparation of Methacrylic Acid Modified Microcrystalline Cellulose and Their Applications in Polylactic Acid: Flame Retardancy, Mechanical Properties, Thermal Stability and Crystallization Behavior. *Cellulose* **2020**, *27*, 2309–2323. [[CrossRef](#)]
18. Matsumoto, K.; Tanaka, T.; Sasada, M.; Sano, N.; Masuyama, K. A Mechanism for Fire Retardancy Realized by a Combination of Biofillers and Ammonium Polyphosphate in Various Polymer Systems. *Cellulose* **2021**, *28*, 3833–3846. [[CrossRef](#)]
19. Fox, D.M.; Temburni, S.; Novy, M.; Flynn, L.; Zammarano, M.; Kim, Y.S.; Gilman, J.W.; Davis, R.D. Thermal and Burning Properties of Poly(lactic acid) Composites Using Cellulose-Based Intumescent Flame Retardants. In *ACS Symposium Series*; ACS Publications: Washington, DC, USA, 2012; Volume 1118, pp. 223–234.
20. Fox, D.M.; Novy, M.; Brown, K.; Zammarano, M.; Harris, R.H.; Murariu, M.; McCarthy, E.D.; Seppala, J.E.; Gilman, J.W. Flame Retarded Poly(lactic acid) Using POSS-Modified Cellulose. 2. Effects of Intumescent Flame Retardant Formulations on Polymer Degradation and Composite Physical Properties. *Polym. Degrad. Stab.* **2014**, *106*, 54–62. [[CrossRef](#)]
21. Yang, W.; Zhao, X.; Fortunati, E.; Dominici, F.; Kenny, J.M.; Puglia, D.; Wang, D.Y. Effect of Cellulose Nanocrystals on Fire, Thermal and Mechanical Behavior of N,N'-Diallyl-Phenylphosphoricdiamide Modified Poly(lactic acid). *J. Renew. Mater.* **2017**, *5*, 423–434. [[CrossRef](#)]

22. Feng, J.; Sun, Y.; Song, P.; Lei, W.; Wu, Q.; Liu, L.; Yu, Y.; Wang, H. Fire-Resistant, Strong, and Green Polymer Nanocomposites Based on Poly(lactic acid) and Core–Shell Nanofibrous Flame Retardants. *ACS Sustain. Chem. Eng.* **2017**, *5*, 7894–7904. [[CrossRef](#)]
23. He, J.; Sun, Z.; Chen, Y.; Xu, B.; Li, J.; Qian, L. Grafting Cellulose Nanocrystals with Phosphazene-Containing Compound for Simultaneously Enhancing the Flame Retardancy and Mechanical Properties of Poly(lactic acid). *Cellulose* **2022**, *29*, 6143–6160. [[CrossRef](#)]
24. Kaci, M.; Aouat, T.; Devaux, E.; Lopez-Cuesta, J.-M. The Effects of Filler Size and Content on the Fire Behavior of Melt-Spun Poly(lactic acid)/Cellulose Bionanocomposite Fibers. In Proceedings of the AIP Conference Proceedings, Ischia, Italy, 12–14 September 2019; Volume 2196, p. 020017.
25. Aouat, T.; Kaci, M.; Devaux, E.; Campagne, C.; Cayla, A.; Dumazert, L.; Lopez-Cuesta, J.-M. Morphological, Mechanical, and Thermal Characterization of Poly(lactic acid)/Cellulose Multifilament Fibers Prepared by Melt Spinning. *Adv. Polym. Technol.* **2018**, *37*, 1193–1205. [[CrossRef](#)]
26. Costes, L.; Laoutid, F.; Khelifa, F.; Rose, G.; Brohez, S.; Delvosalle, C.; Dubois, P. Cellulose/Phosphorus Combinations for Sustainable Fire Retarded Poly(lactide). *Eur. Polym. J.* **2016**, *74*, 218–228. [[CrossRef](#)]
27. Zembouai, I.; Bruzaud, S.; Kaci, M.; Benhamida, A.; Corre, Y.-M.; Grohens, Y.; Lopez-Cuesta, J.-M. Synergistic Effect of Compatibilizer and Cloisite 30B on the Functional Properties of Poly(3-Hydroxybutyrate-Co-3-Hydroxyvalerate)/Poly(lactide) Blends. *Polym. Eng. Sci.* **2014**, *54*, 2239–2251. [[CrossRef](#)]
28. Little, R.W. *Flameproofing Textile Fabrics*; Reinhold: New York, NY, USA, 1947.
29. Nuessle, A.C.; Ford, F.M.; Hall, W.P.; Lippert, A.L. Some Aspects of the Cellulose-Phosphate-Urea Reaction. *Text. Res. J.* **1956**, *26*, 32–39. [[CrossRef](#)]
30. Reeves, W.A.; Perkins, R.M.; Piccolo, B.; Drake, G.L. Some Chemical and Physical Factors Influencing Flame Retardancy. *Text. Res. J.* **1970**, *40*, 223–231. [[CrossRef](#)]
31. Nam, S.; Condon, B.D.; Parikh, D.V.; Zhao, Q.; Cintrón, M.S.; Madison, C. Effect of Urea Additive on the Thermal Decomposition of Greige Cotton Nonwoven Fabric Treated with Diammonium Phosphate. *Polym. Degrad. Stab.* **2011**, *96*, 2010–2018. [[CrossRef](#)]
32. Bocz, K.; Szolnoki, B.; Farkas, A.; Verret, E.; Vadas, D.; Decsov, K.; Marosi, G. Optimal Distribution of Phosphorus Compounds in Multi-Layered Natural Fabric Reinforced Biocomposites. *Express Polym. Lett.* **2020**, *14*, 606–618. [[CrossRef](#)]
33. Decsov, K.; Takács, V.; Marosi, G.; Bocz, K. Microfibrous Cyclodextrin Boosts Flame Retardancy of Poly(lactic acid). *Polym. Degrad. Stab.* **2021**, *191*, 109655. [[CrossRef](#)]
34. Ferrari, A.C.; Robertson, J. Interpretation of Raman Spectra of Disordered and Amorphous Carbon. *Phys. Rev. B* **2000**, *61*, 14095–14107. [[CrossRef](#)]
35. Shafizadeh, F.; DeGroot, W.F. Combustion characteristics of cellulosic fuels. In *Thermal Uses and Properties of Carbohydrates and Lignins*; Elsevier: Amsterdam, The Netherlands, 1976; pp. 1–17.
36. Horrocks, A.R. Developments in Flame Retardants for Heat and Fire Resistant Textiles—the Role of Char Formation and Intumescence. *Polym. Degrad. Stab.* **1996**, *54*, 143–154. [[CrossRef](#)]
37. Schartel, B.; Hull, T.R. Development of Fire-Retarded Materials—Interpretation of Cone Calorimeter Data. *Fire Mater.* **2007**, *31*, 327–354. [[CrossRef](#)]
38. Ghazzawi, Y.M.; Osorio, A.F.; Heitzmann, M.T. The Effect of Fibre Length and Fibre Type on the Fire Performance of Thermoplastic Composites: The Behaviour of Polycarbonate as an Example of a Charring Matrix. *Constr. Build Mater.* **2020**, *234*, 117889. [[CrossRef](#)]
39. Xu, W.; Zhang, B.; Xu, B.; Li, A. The Flame Retardancy and Smoke Suppression Effect of Heptaheptamolybdate Modified Reduced Graphene Oxide/Layered Double Hydroxide Hybrids on Polyurethane Elastomer. *Compos. Part A Appl. Sci. Manuf.* **2016**, *91*, 30–40. [[CrossRef](#)]
40. Xu, W.; Xu, B.; Li, A.; Wang, X.; Wang, G. Flame Retardancy and Smoke Suppression of MgAl Layered Double Hydroxides Containing P and Si in Polyurethane Elastomer. *Ind. Eng. Chem. Res.* **2016**, *55*, 11175–11185. [[CrossRef](#)]
41. Xu, W.; Wang, G.; Liu, Y.; Chen, R.; Li, W. Zeolitic Imidazolate Framework-8 Was Coated with Silica and Investigated as a Flame Retardant to Improve the Flame Retardancy and Smoke Suppression of Epoxy Resin. *RSC Adv.* **2018**, *8*, 2575–2585. [[CrossRef](#)]

**Disclaimer/Publisher’s Note:** The statements, opinions and data contained in all publications are solely those of the individual author(s) and contributor(s) and not of MDPI and/or the editor(s). MDPI and/or the editor(s) disclaim responsibility for any injury to people or property resulting from any ideas, methods, instructions or products referred to in the content.